Journal of
www. biophotonics-journal.org
BIOPHOTONICS

WILEY-VCH

J. Biophotonics **5**, No. 10, 785–792 (2012) / **DOI** 10.1002/jbio.201100132

Journal of BIOPHOTONICS

FULL ARTICLE

Fibrillogenesis of human β_2-microglobulin in three-dimensional silicon microstructures

Sabina Merlo[*,1], *Giuseppe Barillaro*[2], *Francesca Carpignano*[1], *Gloria Silva*[1], *Salvatore Surdo*[2], *Lucanos M. Strambini*[2], *Sofia Giorgetti*[3], *Daniela Nichino*[4], *Annalisa Relini*[4], *Giuliano Mazzini*[5], *Monica Stoppini*[3,6], *and Vittorio Bellotti*[3,6]

[1] Dipartimento di Elettronica, Università di Pavia, Via Ferrata 1, 27100 Pavia, Italy
[2] Dipartimento di Ingegneria dell'Informazione, Elettronica, Informatica, Telecomunicazioni, Università di Pisa, Via G. Caruso 16, 56122 Pisa, Italy
[3] Dipartimento di Medicina Molecolare, Università di Pavia, Via Taramelli 3b, 27100 Pavia, Italy
[4] Dipartimento di Fisica, Università di Genova, Via Dodecaneso 33, 16146 Genova, Italy
[5] IGM-CNR and Dipartimento di Biologia Animale, Università di Pavia, Via Abbiategrasso 207, 27100 Pavia, Italy
[6] Istituto Nazionale di Biostrutture e Biosistemi, Viale Medaglie d'Oro 305, 00136 Roma, Italy

Received 5 December 2011, revised 3 January 2012, accepted 4 January 2012
Published online 27 January 2012

Key words: atomic force microscopy, fluorescence, micromachining, microstructure, silicon, amyloid fibrils

Supporting information for this article is available free of charge under http://dx.doi.org/10.1002/jbio.201100132

The authors describe the interaction of biological nanostructures formed by β_2-microglobulin amyloid fibrils with three-dimensional silicon microstructures consisting in periodic arrays of vertical silicon walls (≈3 μm-thick) separated by 50 μm-deep air gaps (≈5 μm-wide). These structures are of great interest from a biological point of view since they well mimic the interstitial environment typical of amyloid deposition in vivo. Moreover, they behave as hybrid photonic crystals, potentially applicable as optical transducers for label-free detection of the kinetics of amyloid fibrils formation. Fluorescence and atomic force microscopy (AFM) show that a uniform distribution of amyloid fibrils is achieved when fibrillogenesis occurs directly on silicon. The high resolution AFM images also demonstrate that amyloid fibrils grown on silicon are characterized by the same fine structure typically ensured by fibrillogenesis in solution.

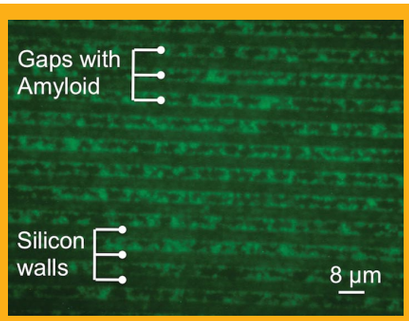

Fluorescence microscopy (100×) image of the silicon photonic crystal (top view) filled with P32G β_2-m directly polymerized *in situ*.

1. Introduction

Amyloidosis is a pathology known from more than a century, but in the last decade has attracted an extraordinary medical interest because the deposition of amyloid fibrils and amyloid-like fibrils is considered a causative or co-causative agent of diseases of relevant social and economical impact such as Alzhei-

* Corresponding author: e-mail: sabina.merlo@unipv.it, Phone: +39 0382 985202, Fax: +390382422583

Journal of
BIOPHOTONICS

mer's, systemic amyloidoses and Parkinson's [1]. For this reason, the structure and the biology of the amyloid fibrils are under extensive investigation in many laboratories and several methods suitable for the conversion of this protein from the soluble to the fibrillar state have been discovered [2–5]. In this framework, new technologies aimed at the investigation of proteins, linked to surfaces in micro-volumes, are also emerging. Label-free sensing methods, such as surface plasmon resonance and quartz-crystal microbalances, all based on planar devices, have been developed and applied to probe the growth of amyloid fibrils and their interaction with small molecules [6–10]. The development of methods for the immobilization of amyloid fibrils on silicon surfaces of three-dimensional structures and for the optical analysis of the immobilized molecules would be highly valuable.

In this paper, we investigate the use of a silicon micromachined structure as a three-dimensional supporting matrix for biological nanostructures, which is also potentially useful as optical transducer in a label-free biosensor, in particular for monitoring amyloid fibrils formation. The silicon microstructure consists in a periodic array of parallel ≈3 μm-thick silicon walls separated by ≈5 μm-wide, 50 μm-deep air gaps, fabricated by electrochemical micromachining (ECM) of (100)-oriented *n*-type silicon wafers. Electrochemical micromachining is a powerful technology for the low-cost fabrication of vertical, high aspect-ratio (about 17 in this work) microstructures with high flexibility. The periodic arrangement of silicon walls and air gaps (dielectric materials) along one direction gives rise to an artificial material, known as high-order Bragg reflectors or one-dimensional hybrid photonic crystals [11]. They are characterized by the presence of photonic bandgaps, corresponding to wavelength intervals in which the propagation of the electromagnetic field inside the material is prohibited and reflectivity in direction orthogonal to the silicon walls is very high. The spectral position of the bandgaps strongly depends on the distribution and refractive index of the material filling the gaps. In our previous papers, we demonstrated [11, 12] that vertical periodic microstructures fabricated by electrochemical micromachining of silicon exhibit good uniformity and optical quality surfaces, since roughness is limited to peak-to-valley variations of a few tens of nanometers, yielding a quality factor of ≈ 3000 for the reflectivity notch at 1.55 μm. Such micromachined structures can be proposed as building blocks for high-sensitivity label-free biosensors due to the possibility of using reflections from multiple periodic surfaces – instead of reflection from just a single surface as it usually happens for planar structures – for the detection of biological matter immobilized on the surfaces or trapped between the silicon plane, as schematically reported in Figure 1(a). We recently performed [13, 14] reflectivity measurements after infiltration of these silicon structures with liquids (water, ethanol and isopropanol) and verified their optofluidic properties such as good mechanical stability upon liquid insertion/extraction. We also introduced a sensitivity parameter as the variation of the center wavelength of the photonic bandgaps as functions of refractive index variations of the liquid filling the gaps, and found an experimental value of approximately 1000 nm/RIU (RIU = refractive index unit) in agreement with theoretical results [13, 14].

In view of our final aim to develop a new tool for optically monitoring the kinetics of amyloid fibrils formation, objective of this work is to demonstrate that a uniform distribution of amyloid fibrils, characterized by the same fine morphology typically ensured by fibrillogenesis in solution, can be effectively achieved also in the narrow and deep gaps of the vertical, one-dimensional photonic crystal that simulate the interstitial environment typical of amyloid

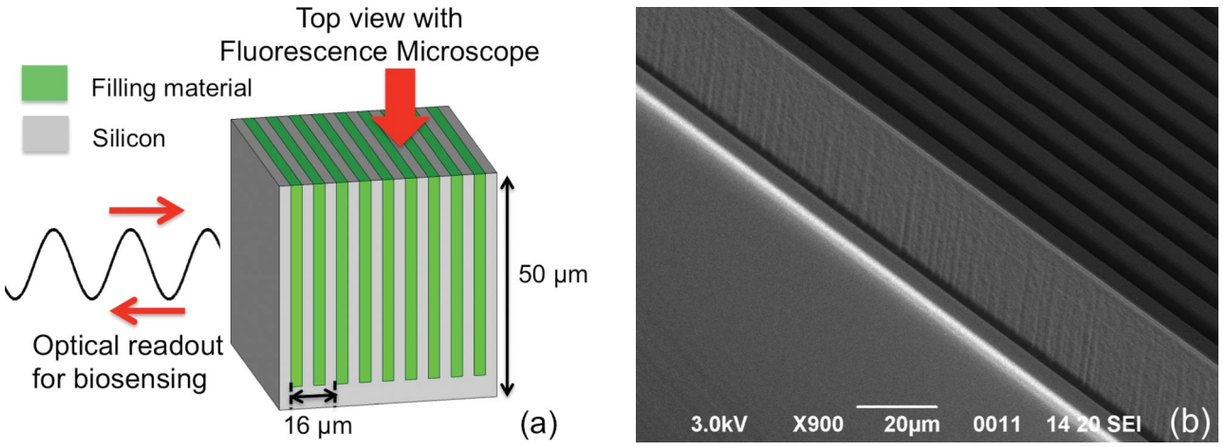

Figure 1 (online color at: www.biophotonics-journal.org) (**a**) Schematic drawing of the periodic array of silicon walls; (**b**) Scanning Electron Microscopy image of the three-dimensional silicon microstructure.

deposition *in vivo* [15]. A uniform distribution of biological material in the gaps is expected to be important for fully exploiting the photonic crystal potential, mainly related to an efficient cumulative effect due to the superposition and interference of optical waves reflected at the various interfaces within the micromachined structure.

In this paper, we report the results of various tests that have been performed to investigate the interaction of the highly amyloidogenic variant of human β_2-microglobulin (P32G β_2-m), used as a prototypical amyloidogenic protein, with flat, polished silicon surfaces, and with three-dimensional microstructures, such as vertical, high aspect-ratio one-dimensional photonic crystals fabricated by ECM. Atomic force and fluorescence microscopy analyses show that a uniform distribution of amyloid fibrils on the silicon surface is observed only in the case of *in situ* polymerization, whereas high resolution images collected by atomic force microscopy (AFM) demonstrate that the fine texture of amyloid fibrils is not affected by the presence of silicon during polymerization.

2. Materials and methods

2.1 Silicon microstructure fabrication

The fabrication of the three-dimensional silicon microstructures used in the experiments was performed by means of the electrochemical micromachining technology according to the process detailed in [11]. The starting material was a 675 μm-thick n-doped silicon wafer, (100) oriented, resistivity of 3–8 $\Omega \cdot$ cm, with a 100 nm-thick thermally grown silicon dioxide layer on its top. A square array of 1 cm-long parallel straight lines, with a width $d = 4$ μm and a pitch $p = 8$ μm, was defined in the center of a 2 cm × 2 cm silicon die by means of a standard lithographic step. A BHF (Buffered Hydrofluoric Acid) etch and a KOH (Potassium Hydroxide) etch were used to transfer the pattern in the silicon dioxide layer and in the silicon substrate surface, respectively. The KOH etch formed full V-grooves that were used as initial seeds for the controlled electrochemical etching of silicon. Electrochemical etching of silicon was performed in a HF-based solution ($HF:H_2O = 5:95\%$ by volume, with the addition of 1000 ppm of Sodium Lauryl Sulfate (SLS) used as surfactant) and used to fabricate deep regular trenches (air gaps) in the patterned substrate over a circular etching area of 0.66 cm^2. The etching voltage V_{etch} was set to a constant value of 3 V for the entire etching process, while the etching current I_{etch} was set to an initial value $I_{etch0} = 26.41$ mA and properly reduced with time during the etching process in order to obtain trenches with constant width $w = 5$ μm over the whole etching depth (nominal porosity $P = w/p = 62.5\%$). The etching time $t_{etch} = 2400$ s was chosen to fully etch 55 μm-deep trenches. After the electrochemical etching, a chemical etching step aimed to the removal of the surfactant from the silicon surface and a subsequent drying step aimed to the evaporation of the liquid filling the trenches were performed. A Scanning Electron Microscope (SEM) image of the silicon microstructure used in the experiments is reported in Figure 1(b). Flat 1 × 1 cm silicon dice were obtained from polished silicon wafers, without silicon dioxide layer on top, with same thickness, orientation, and resistivity.

2.2 Fibrillogenesis in suspension

For fibrillogenesis in suspension, a standard protocol was followed [3]. Recombinant β_2-microglobulin presenting the P32G mutation, at a concentration of 40 μM, was incubated for 72 h at 37 °C under agitation at 250 r.p.m. in 25 mM sodium phosphate buffer (pH 7.0) in the presence of heparin 100 μg/ml and preformed β_2-m fibrils seeds at a concentration of 2.5 μg/ml [3]. These pre-polymerized fibril samples were centrifuged and washed in water to remove phosphate residuals before deposition on silicon dice. This step avoided the formation, upon sample dehydration, of phosphate crystals that would have prevented a clear identification and visualization of fibril aggregates. Quantification of amyloid formation was performed with Thioflavin T (ThT) according to [16]. ThT (Sigma-Aldrich) concentration was 10 μM in 50 mM glycine/NaOH buffer, pH 8.5. A LS50 Perkin Elmer spectrofluorimeter was used for the measurements, with excitation at 445 nm and emission collected at 480 nm, with slits set at 5 nm.

2.3 Interaction of silicon dice with pre-polymerized fibril samples

An aliquot (50 μl) of pre-polymerized fibrils (P32G β_2-m at $T1 = 72$ h) was gently placed on top of different silicon devices, placed in a multi well plate. Incubation on silicon occurred for approximately 6 h; during this time, the plate was maintained at room temperature in a 100% humid environment to avoid dehydration. Reference samples were prepared placing un-polymerized proteins at the same concentration (P32G β_2-m at $T0 = 0$) on a second device.

Journal of
BIOPHOTONICS

2.4 Fibrillogenesis on silicon dice

In order to achieve fibrillogenesis directly on silicon, recombinant P32G β_2-m at a concentration of 40 μM was incubated in contact with the silicon dice, in a vial, for 5 days at 37 °C under agitation at 250 r.p.m. in water (without sodium phosphate), in the presence of heparin 100 μg/ml and preformed β_2-m fibrils seeds at a concentration of 2.5 μg/ml. Silicon surfaces were not subjected to any specific preliminary treatment, except for electrochemical micromachining in case of three-dimensional structures.

2.5 Fluorescence microscopy analysis

After removal of the excess solutions from the top of the silicon devices, all the samples were stained with ThT (1% (w/v) solution in water) for 10 min at room temperature. The samples were then washed with 1% acetic acid for 5 min and, finally, rinsed in water. Silicon dice were transferred on glass slides and covered with cover slips for microscopy observation.

All samples were observed with an Olympus BX51 microscope with standard fluorescence equipment (HBO100/2 lamp). Blue excitation specific for the ThT fluorochrome was performed with a band-pass (BP 450–480 nm) excitation filter through a dichroic mirror DM500 combined with a LP 515 nm as barrier filter. Fluorescence microphotographs at 40× and 100× (oil immersion) magnifications were taken using an Olympus Camedia C-4040 digital camera.

2.6 Atomic force microscopy analysis

For AFM imaging, P32G β_2-m samples deposited or directly polymerized on silicon were allowed to dry overnight. Atomic force microscopy measurements were performed in air using a Dimension 3100 scanning probe microscope equipped with a G scanning head (maximum scan size 100 μm) and driven by a Nanoscope IIIa controller and a Multimode SPM, equipped with "E" scanning head (maximum scan size 10 μm) and driven by a Nanoscope V controller, (Digital Instruments, Bruker AXS GmbH, Karlsruhe, Germany). Images were acquired in tapping mode in air using single beam uncoated silicon cantilevers (type OMCL-AC160TS, Olympus, Tokyo, Japan). The drive frequency was between 280 and 320 kHz and the scan rate was between 0.5 and 2.0 Hz. The Nanoscope software was used to evaluate aggregate heights from the cross-sections of topographic images and to calculate the surface roughness, defined as the root mean square average of height deviations from the mean data plane.

3. Results and discussion

All the different combinations of fibrillar nanostructures and silicon devices were analyzed under fluorescence microscopy whereas fibrillar nanostructures on flat silicon were also investigated by means of atomic force microscopy. Results of these analyses are discussed in the following.

3.1 Fluorescence microscopy imaging of amyloid fibrils on flat silicon

Fluorescence microscopy was used for the analysis of all the silicon devices used as supports for proteins. As reported in the literature [16–19], the fluorescence quantum yield of ThT is greatly affected by the solvent viscosity and the rigidity of the microenvironment, so that this fluorochrome has thus been used for recognition of aggregated amyloid in vitro. ThT exhibits an absorption peak at 450 nm (blue) and a great increase in the emission fluorescence is observed upon binding to amyloid fibrils [18]. We first examined amyloid fibrils that were pre-polymerized in suspension following the protocol described in (2.2) and, then, incubated on flat silicon for a few hours. As shown in the fluorescence image reported in Figure 2(a), the silicon substrate appears to be ir-

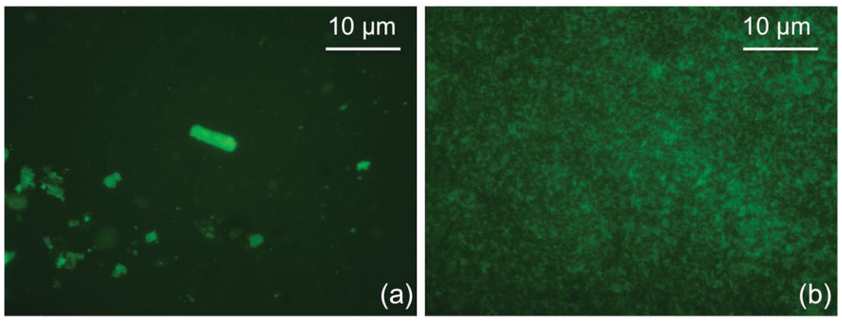

Figure 2 (online color at: www.biophotonics-journal.org) Fluorescence images taken at 100× magnification on flat silicon dice. (**a**) Pre-polymerized sample of P32G β_2-m 40 μM placed on flat silicon; (**b**) P32G β_2-m 40 μM directly polymerized on flat silicon.

regularly and scarcely covered by fibrils. In order to improve surface coating, fibrillogenesis was then performed directly on flat silicon dice (as described above). A typical fluorescence image observed on these samples is shown in Figure 2(b); in this case, a significantly improved covering of the silicon surface by amyloid fibrils with a fine texture is observed, thus suggesting that in situ fibrillogenesis, using standard protein concentration and incubation time, is an effective method to obtain a uniform fibril distribution on silicon surfaces.

3.2 AFM imaging of amyloid fibrils on flat silicon

Tapping mode AFM was employed to investigate the morphology and the structural details of fibrillar samples on flat silicon substrates. Figure 3 compares the surface plots obtained from a sample of preformed P32G β_2-m fibrils deposited on silicon (Figure 3(a)) and from fibrils directly grown on the silicon substrate (Figure 3(b)). The AFM analysis clearly shows that fibril deposition on silicon results into an irregular coverage of the substrate. The centrifugation procedure required to remove salts from the sample before deposition gives rise to the formation of tight fibril networks or clusters which after deposition are found to be surrounded by large portions of bare substrate (Figures 3(a) and S1(a)). On the other hand, *in situ* polymerization, not requiring the centrifugation step, gives rise to a uniform distribution of aggregates on the substrate (Figures 3(b) and S1(c)). When inspected at higher resolution, both preformed and grown *in situ* fibrils display a similar structure (Figure 4). The typical fibril length is between 300 nm and 1 μm, while the height of the thinnest single fibrillar structures, which can be thought of as the constituent units of the larger aggregates, is about 3 nm. The calculation of surface roughness from the data reported in Figure 3(a) and (b) yields roughness values of 23 nm and 15 nm, respectively, for the same surface area of 9×9 μm, thus indicating that the sample surface texture is smoother in the case of fibrils grown *in situ*. Therefore, *in situ* polymerization is a successful strategy to obtain a uniform coverage of the substrate without altering the fibril structural features.

3.3 Fluorescence microscopy imaging of amyloid fibrils on microstructured silicon

Interaction between amyloid fibrils and silicon three-dimensional microstructures was investigated by means of fluorescence microscopy. Initially, we

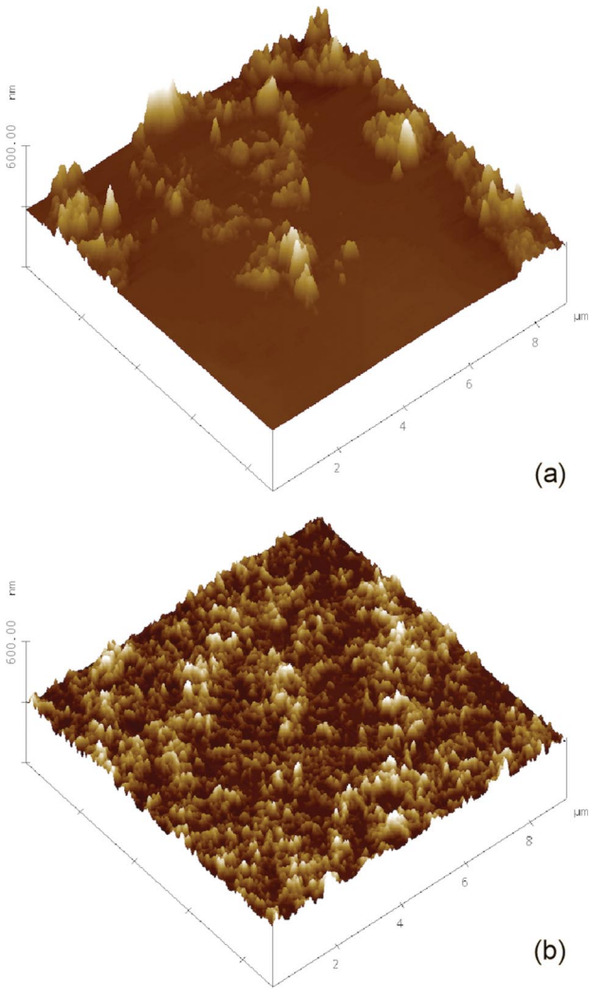

Figure 3 (online color at: www.biophotonics-journal.org) Surface plots of tapping mode AFM images (height data) of P32G β_2-m fibrils (**a**) preformed in solution and then deposited on flat silicon and (**b**) directly grown on the flat silicon substrate.

analyzed pre-polymerized amyloid fibrils incubated for 6 h in the three-dimensional micromachined silicon dice. Bright fluorescence emission was observed coming from the gaps of devices filled with the polymerized P32G β_2-m (P32G β_2-m at $T1 = 72$ h), as shown in Figure 5(b), where fibrillar aggregates are also visible as bright green dots scattered in the silicon matrix. On the other hand, fluorescence from the gaps occupied by the un-polymerized P32G β_2-m (P32G β_2-m at $T0 = 0$) is very weak, as observed in Figure 5(a). In all the images of Figure 5, silicon walls appear as dark stripes since ThT does not bind to silicon. Finally, a typical fluorescence image resulting from fibrillogenesis directly occurred on three-dimensional silicon platforms is reported in Figure 5(c), where uniform filling of the gaps is clearly

Journal of
BIOPHOTONICS

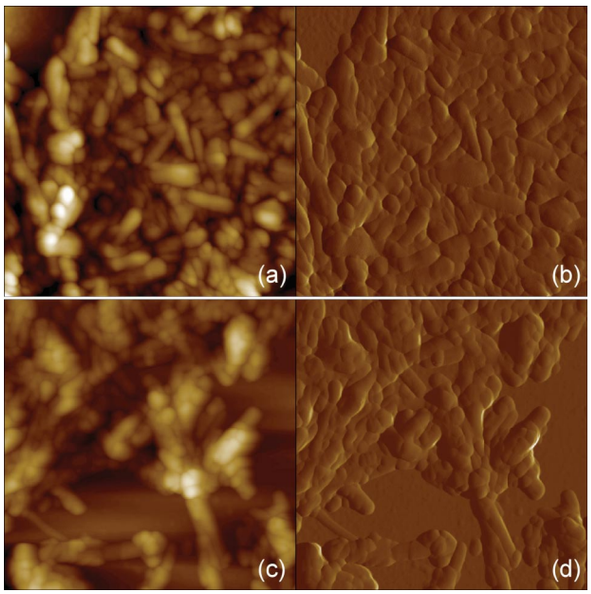

Figure 4 (online color at: www.biophotonics-journal.org) Tapping mode AFM images at high magnification of pre-formed P32G β_2-m amyloid fibrils deposited on silicon (**a**, **b**) and P32G β_2-m amyloid fibrils directly grown on silicon (**c**, **d**). Scan size 750 nm. (**a**, **c**) height data, Z range 30 nm (**a**) and 80 nm (**c**); (**b**, **d**) amplitude data.

visible. In particular, the morphology of the protein texture observed in the gaps between silicon walls (Figure 5(c)) resembles the shape recorded on flat silicon (Figure 2(b)). This is, to our knowledge, the first report of amyloid fibrils directly grown in a three-dimensional silicon micromachined structure, also suitable for future label-free assays. Preliminary data collected with confocal fluorescence microscopy indicate that, with the tested protocol, the gaps are filled up to a depth of 15 μm from the top of the walls. This depth is compatible with the fiberoptic instrumental setup, described in [12], for performing spectral reflectivity measurements with high spatial resolution. Future work will be, anyway, also devoted to improve the depth of filling.

4. Conclusion

Amyloid diseases are emerging as an unmet and highly challenging medical problem because their frequency is growing in parallel with the population ageing and therapeutic tools are limited and in many cases ineffective. Inhibition of protein aggregation is a prominent goal of any effective therapy, and the discovery of new inhibitors requires the assessment of methods of fibrillogenesis, suitable for high-throughput screening of new ligands, and satisfying

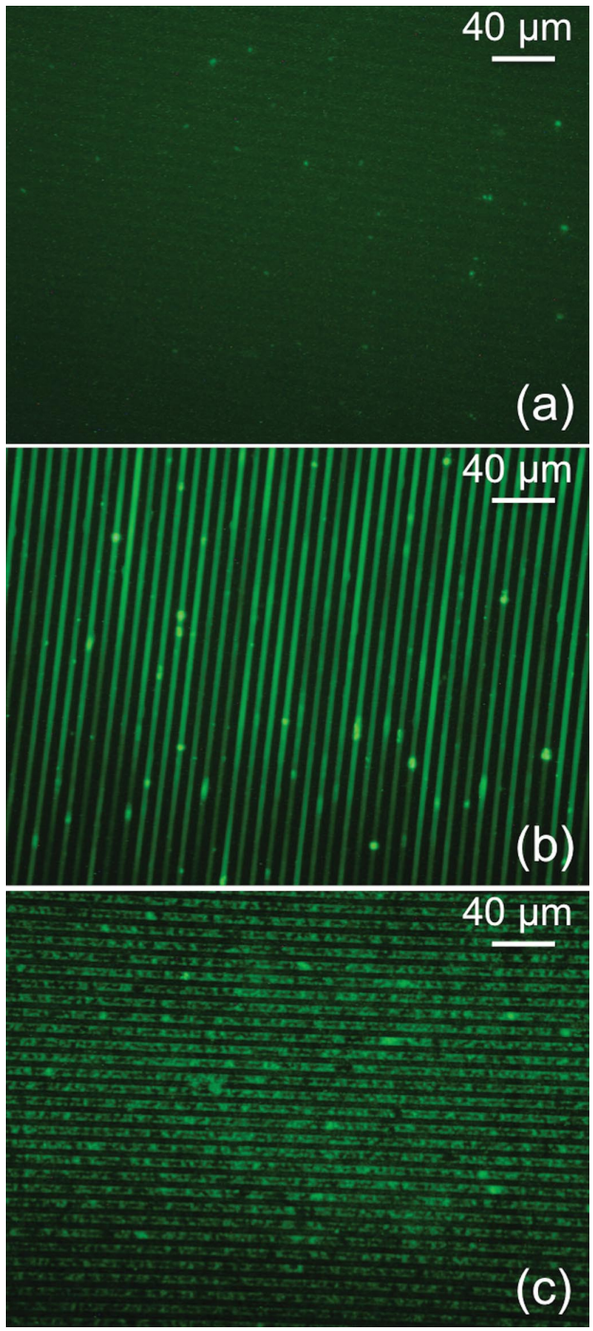

Figure 5 (online color at: www.biophotonics-journal.org) Comparison between fluorescence microscopy (40×) images of three-dimensional silicon devices (top views) filled with P32G β_2-m 40 μM in different conditions of fibrillogenesis. (**a**) Gaps filled with un-polymerized P32G β_2-m (P32G β_2-m at $T0 = 0$); (**b**) gaps filled with pre-polymerized P32G β_2-m in suspension (P32G β_2-m at $T1 = 72$ h); (**c**) P32G β_2-m directly polymerized on silicon.

criteria of sensitivity, specificity and compatibility with the physiologic environment. Our data suggest that microstructured silicon is an excellent material for the preparation of devices in which the conversion of globular protein precursor into polymeric fibril occurs homogeneously on the silicon surface. The fibrils maintain the structural morphology of natural fibrils. Miniaturization of volumes, functionalization of the silicon surface and the wide range of spectroscopic compatibility of silicon is extremely encouraging in pursuing the design of a silicon biochip for monitoring protein fibrillogenesis in microcavities suitable for mimicking physicochemical characteristics of the natural environment of amyloidogenesis which is the tissue's extracellular matrix.

New technologies are arising for the investigation in micro- and nano-volumes of proteins linked to silicon surfaces. The amyloid fibrils certainly represent a protein entity in which the development of a system of surface immobilization and on-line analysis of the optical properties of the immobilized molecule would be particularly valuable. In the recent years several new techniques of label-free optical detection have been exploited in the field of protein chemistry. We are working on a new strategy for monitoring fibril growth in real-time and quantifying the effect on fibrils of other molecular species combining a microstructured device, obtained by silicon micromachining, with an optical readout, based on refractive index variations in the gaps among the silicon walls, induced by the biological samples. Future work will thus devoted to label-free detection with a fiberoptic readout, exploiting the properties of the artificial bandgap material.

Acknowledgements This work was partially supported by the CARIPLO Foundation, the Italian Ministry of University and Research and the CARIGE Foundation. Currently, F. Carpignano and S. Surdo hold a fellowship funded by Fondazione Alma Mater Ticinensis, Pavia, Italy.

Supplementary material: Supplementary data associated with this article can be found in the online version at www. biophotonics-journal.org.

Sabina Merlo is Associate Professor at the Department of Electronics of the University of Pavia.

Giuseppe Barillaro is permanent Researcher and Assistant Professor at the Department of Information Engineering of the University of Pisa.

Francesca Carpignano is enrolled in the Ph.D. program in Bioengineering and Bioinformatics at the University of Pavia.

Gloria Silva is enrolled in the Ph.D. School in Electronics, Computer Science and Electrical Engineering at the University of Pavia.

Salvatore Surdo is PhD student in Information Engineering at the Information Engineering Department of the University of Pisa.

Lucanos Marsilio Strambini holds a post doctorate position at the Information Engineering Department of the University of Pisa.

Sofia Giorgetti is a Researcher at the Department of Molecular Medicine of the University of Pavia.

Daniela Nichino holds a post-doc collaboration contract at the Department of Physics of the University of Genova.

Annalisa Relini is permanent Researcher and Assistant Professor at the Department of Physics of the University of Genova.

Giuliano Mazzini is Senior Researcher in the Section of Cytochemistry and Cytometry of the Institute of Molecular Genetics, within the Italian CNR (National Research Council) in Pavia.

Monica Stoppini is Associate Professor at the Department of Molecular Medicine of the University of Pavia.

Vittorio Bellotti is Full Professor at the Department of Molecular Medicine of the University of Pavia.

References

[1] G. Merlini and V. Bellotti, N. Engl. J. Med. **349**, 583–596 (2003).
[2] N. M. Kad, N. H. Thomson, D. P. Smith, D. A. Smith, and S. E. Radford, J. Mol. Biol. **313**, 559–571 (2001).
[3] S. Giorgetti, S. Raimondi, K. Pagano, A. Relini, M. Bucciantini, A. Corazza, F. Fogolari, L. Codutti, M. Salmona, P. Mangione, L. Colombo, A. De Luigi, R. Porcari, A. Gliozzi, M. Stefani, G. Esposito, V. Bellotti, and M. Stoppini, J. Biol. Chem. **286**, 2121–2131 (2011).

[4] M. Zhu, P. O. Souillac, C. Ionescu-Zanetti, S. A. Carter, and A. L. Fink, J. Biol. Chem. **277**, 50914–50922 (2002).
[5] A. Relini, S. De Stefano, S. Torrassa, O. Cavalleri, R. Rolandi, A. Gliozzi, S. Giorgetti, S. Raimondi, L. Marchese, L. Verga, A. Rossi, M. Stoppini, and V. Bellotti, J. Biol. Chem. **283**, 4912–4920 (2008).
[6] T. P. J. Knowles, W. Shu, G. L. Devlin, S. Meehan, S. Auer, C. M. Dobson, and M. E. Welland, Proc. Natl. Acad. Sci. U.S.A. **104**, 10016–10021 (2007).
[7] I. Maezawa, H. S. Hong, R. Liu, C. Y. Wu, R. H. Cheng, M. P. Kung, H. F. Kung, K. S. Lam, S. Oddo, F. M. LaFerla and L.W. Jin, J. Neurochem. **104**, 457–468 (2008).
[8] D. A. White, A. K. Buell, C. M. Dobson, M. E. Welland, and T. P. J. Knowles, FEBS Lett. **583**, 2587–2592 (2009).
[9] A. K. Buell, C. M. Dobson, T. P. J. Knowles, and M. E. Welland, Biophys. J. **99**, 3492–3497 (2010).
[10] A. K. Buell, E. K. Esbjorner, P. J. Riss, D. A. White, F. I. Aigbirhio, G. Toth, M. E. Welland, C. M. Dobson, and T. P. J. Knowles, Phys. Chem. Chem. Phys. **13**, 20044–20052 (2011).
[11] G. Barillaro, L. M. Strambini, V. Annovazzi-Lodi, and S. Merlo, IEEE J. Sel. Top Quantum Electron. **15**, 1359–1367 (2009).
[12] G. Barillaro, S. Merlo, S. Surdo, L. M. Strambini, and F. Carpignano, IEEE Photonics J. **2**, 981–990 (2010).
[13] G. Barillaro, S. Merlo, and L. M. Strambini, Opt. Lett. **34**, 1912–1914 (2009).
[14] G. Barillaro, S. Merlo, S. Surdo, L. M. Strambini, and F. Carpignano, Microfluid Nanofluidics. **12**, 545–552 (2012).
[15] V. Bellotti, and F. Chiti, Curr. Opin. Struct Biol. **18**, 771–779 (2008).
[16] H. LeVine, Protein Sci **2**, 404–410 (1993).
[17] A. Hawe, M. Sutter, and W. Jiskoot, Pharm. Res. **25**, 1487–1499 (2008).
[18] N. R. Nilsson, Methods **34**, 151–160 (2004).
[19] T. Ban, D. Hamada, K. Hasegawa, H. Naiki, and Y. Goto, J. Biol. Chem. **278**, 16462–16465 (2003).

